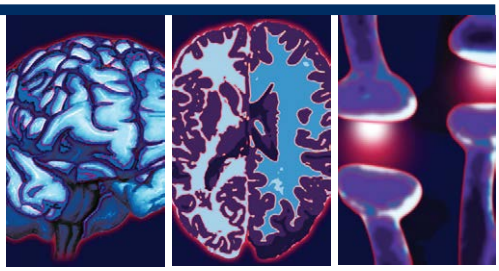

Disrupted Resting-State Brain Functional Architecture in Amphetamine-Type Stimulant Abusers

Qun Chen[1], Dang Zheng[2,3,4], Shaojuan Cui[5], Kai-Juan Yan[1,2],Chen-xiao Fan[6], Guo-fu Zhang[1,2], Le Xiao[1,2], Yan Li[1], Xiao-fei Yuan[1,2], Kankan Xie[7], Yaqiong Li[1,2], Xiao-nian Luo[1,2], Yuan Zhou[2,3,4], Zhan-Jiang Li[1,†]

ABSTRACT

Background:

The abuse of amphetamine-type stimulants has continued to increase, leading to new challenges to human health. However, the effects of the abuse of amphetamine-type stimulants on brain functional networks are unclear. The aim of the current study was to use resting-state functional magnetic resonance imaging (rs-fMRI), a technique that is used to study the brain's intrinsic functional organization, to characterize the brain functional architecture influenced by amphetamine-type stimulant abuse.

Methods:

The present study recruited seventeen male amphetamine-type stimulant abusers (ATSAs) and twenty-two healthy male controls. We used degree centrality (DC) and seed-based resting-state functional connectivity (RSFC) analyses to identify brain functional architecture differences between ATSAs and healthy controls (HCs).

Results:

The ATSA group showed a decreased DC, especially in a large cluster including the right anterior, middle, and posterior insula. Furthermore, seed-based RSFC analyses revealed decreased functional connectivity in a network composed of the right posterior insula, medial prefrontal cortex, visual and sensorimotor cortices as well as in a network composed of the right middle insula and visual cortices in the ATSA group.

Conclusion:

These results provide evidence that the resting-state brain functional architecture is disrupted in amphetamine-type stimulant abusers from a network perspective.

Keywords:

Resting-state functional connectivity , Amphetamine-type stimulants abuse, Insula, Medial prefrontal cortex, Heroin abusers

[1]The National Clinical Research Center for Mental Disorders & Beijing Key Laboratory of Mental Disorders, Beijing Anding Hospital, Capital Medical University, Beijing, P. R. China

[2]CAS Key Laboratory of Behavioral Science, Institute of Psychology, Beijing, PR China

[3]Department of Psychology, University of Chinese Academy of Sciences, Beijing, PR China

[4]Magnetic Resonance Imaging Research Center, Institute of Psychology, Chinese Academy of Sciences, Beijing, PR China

[5]Department of Psychology, Beijing Tongren Hospital, Capital Medical University, Beijing, PR China

[6]Jinhua The Second Hospital, Zhejiang, PR China

[7]The Third Hospital of Chaoyang District, Beijing, PR China

[†]Author for correspondence: Zhan-jiang Li, M.D., Ph.D, The National Clinical Research Center for Mental Disorders & Beijing Key Laboratory of Mental Disorders, Beijing Anding Hospital, Capital Medical University, No. 5 Ankang Hutong, Deshengmen Wai, Xicheng District, Beijing (100088), P. R. China, email: izhj8@ccmu.edu.cn

Introduction

Drug abuse is a severe public issue that poses a global threat to human health, social stability, and economic development. Worldwide, the proportion of people abusing amphetamine-type stimulants experiences a large growth every year (http://www.unodc.org/wdr2016/). For example, in China, the proportion of amphetamine-type stimulant abusers (ATSAs) exceeded that of heroin abusers for the first time in 2014 (http://www.nncc626.com/2015-06/24/c_127945747_2.htm), and the proportion of ATSAs has maintained a continuous upward trend over the past five years. In comparison with the abuse of opioid drugs, such as heroin, abuse of amphetamine-type stimulants (a group of drugs whose principal members include amphetamine and methamphetamine) is a new trend [1]. Abuse of synthetic mephedrone, whose derivatives are similar to amphetamine, has been found to cause psychotic episodes of hallucinations, aggression, paranoia, suicidal thoughts or impulses, and homicidal tendencies [2]. Moreover, amphetamine-type stimulants lead to extensive neural damage and abnormal functional and structural organization of the brain [3-5]. The structural abnormalities are mainly related to a smaller grey matter volume within all cerebral cortices (temporal, frontal, occipital, and parietal lobe) and increased striatal and basal ganglia gray matter volume, as well as the invariably accompanied trend of increased white matter volume [5]. Multiple brain region abnormality (e.g., frontal and temporal systems) contributes to amphetamine users' impaired cognitive abilities, such as episodic memory, to some extent [4], and prefrontal and insular hypoactivtion during a decision-making task can predict amphetamine relapse [6].

Resting-state functional magnetic resonance imaging (rs-fMRI) has provided a new venue to understand the brain's intrinsic functional organization [7-10]. Rs-fMRI involves analysis of spontaneous brain function using blood oxygen level-dependent contrasts in the absence of a task, rendering it suitable for clinical applications [11]. Rs-fMRI has been successfully applied to the characterization of brain function disturbances in substance-dependent populations, including individuals addicted to heroin [12-15], nicotine [16-19], and cocaine [20,21]. These rs-fMRI findings provide evidence that regions related to reward, memory and learning, cognitive control, motivation, and salience evaluation are involved in addiction [22].

Compared with opiate addiction, there are fewer imaging studies focused on the abuse of amphetamine-type stimulants [23-26]. Considering that the most serious frequently reported problems by ATSAs were psychological rather than physical [27], it is possible that amphetamine-type stimulants have specific effects on brain function. In healthy volunteers, acute effects of 3,4-methylenedioxymethamphetamine (MDMA) on spontaneous brain function have been found, specifically as indicated by decreased resting-state functional connectivity (RSFC) between the ventral medial prefrontal cortex (vMPFC) and medial temporal lobe (MTL) and between the vMPFC and posterior cingulate cortex (PCC) as well as increased RSFC between the amygdala and hippocampus [23]. In amphetamine-type stimulant abusers, Kohno, *et al.* found increased RSFC related to the midbrain, and they also found a negative correlation between the midbrain RSFC and right dorsolateral prefrontal cortex (DLPFC) activity that was modulated by risk during a decision-making task in these abusers [28]. Dean, *et al.* found that denial (a lack of recognition that a problem exists and needs to be changed) in methamphetamine users was associated with functional connectivity between the frontal lobe and rostral anterior cingulate [26]. These studies indicate that rs-fMRI can detect changes in the brains of amphetamine-type stimulant abusers. However, the regions influenced by amphetamine-type stimulants are inconsistent across studies.

In this study, we aimed to identify differences between the resting-state brain functional architecture of ATSAs and healthy controls (HCs) using a method combing whole-brain exploration of functional networks and seed-based RSFC. We first used voxel-wise degree centrality (DC) analysis, a method that is widely used to detect changes in resting-state functional networks [29-33], to characterize the functional relationships of a given voxel (node) within the entire connectivity matrix of the brain [29,34,35]. Due to the inconsistent findings of previous rs-fMRI studies of ATSAs, this examination of voxel-wise DC allowed us to identify brain regions that might be influenced by amphetamine-type stimulants without requiring a priori selection of nodes or networks of interest. Next, seed-based RSFC analysis was used to further reveal the details of the functional networks that were associated with the identified regions [29,33].

Materials and methods

■ Subjects

Male ATSAs (n = 17) were recruited from the Wuhan Mental Health Centre affiliated with the Huazhong University of Science and Technology during the period from October 2012 to December 2012. Healthy male controls (n = 22) were recruited from the local community and Huazhong University of Science and Technology using posted advertisements. The inclusion criteria for both groups were as follows: 18-40 years of age, male, at least 9 years of education, normal or corrected-to-normal vision and hearing, and no reported history of neurological problems, severe head injuries, or ophthalmic diseases. HC subjects were screened by telephone interviews and excluded when they met the current or past criteria for any Axis I psychiatric disorder according to the Diagnostic and Statistical Manual for Mental Disorders, 4th Edition (DSM-IV) [36]. All enrolled ATSAs met the DSM-IV criteria for drug dependence and were assessed using the Chinese version of the Addiction Severity Index (ASI-C) [37], in which clinicians assessed each participant on seven potential problem areas: medical, employment/support status, alcohol, drug, legal, family/social, and psychiatric [38]. Furthermore, the enrolled ATSA participants all had used amphetamine-type stimulants for more than one year, and the accumulated dosage of the amphetamine-type stimulants they used was above 50g. Based on self-reports of these abusers, among the 17 ATSAs, 8 participants used methamphetamine only and 9 participants used two or three amphetamine-type stimulants, such as methamphetamine, ecstasy or ketamine. None of the ATSAs and HCs had a history of abuse or dependence on other substances, with the exceptions of nicotine, caffeine, and alcohol. All of the ATSAs were inpatients, so they were in a state of withdrawal from any substance, including amphetamine-type stimulants, nicotine, caffeine, and alcohol. One ATSA and one HC subject were later excluded from the study because of excessive head motion during the fMRI scan (see the following section). This study was approved by the Ethics Committee of Wuhan Mental Health Centre, and all experiments were performed in accordance with relevant guidelines and regulations. All participants or families of ATSAs provided informed consent before participation.

■ MRI data acquisition

Images were acquired with a 1.5 Tesla MRI scanner (Model: GE Signa HDxt) in Zhongshan Hospital, Wuhan City, Hubei Province, China. Whole-brain functional scans were collected in 33 axial slices using an echo-planar imaging (EPI) sequence (repetition time = 3000 ms; echo time = 40 ms; flip angle= 90°; matrix = 64 × 64; field of view = 220 × 220 mm^2; slice thickness = 3 mm; slice gap = 1 mm). Each functional run contained 180 volumes. High-resolution T1-weighted images were acquired in a sagittal orientation employing a fast SPGR sequence (repetition/echo time = 9.176/2.956 ms; flip angle = 20°; slice thickness = 1.2 mm (no gap); number of slices = 128).

■ Data preprocessing

Unless otherwise stated, all preprocessing was performed using the Data Processing Assistant for Resting-State fMRI (DPARSF 2.3, http://www.restfmri.net) [39], which is based on the Statistical Parametric Mapping (SPM8) program (http://www.fil.ion.ucl.ac.uk/spm) and the Resting-State fMRI Data Analysis Toolkit (REST 1.8, http://www.restfmri.net) [40]. Prior to preprocessing, the first 10 volumes were discarded to allow for signal stabilization. The remaining volumes acquired from each subject were corrected for differences in slice acquisition times. The resultant images were then realigned to correct for small movements that occurred between scans. Based on the recorded motion correction estimates, subjects with a maximum displacement of more than 3 mm (in the x, y, or z direction) or more than 3° of angular rotation about any axis for any of the 170 volumes were excluded from the study. Based on these criteria, one amphetamine-type stimulant abuser and one healthy volunteer were excluded from the analyses. The realigned EPI images were co-registered to individual T1-weighted structural images. The transformed structural images were then segmented into gray matter, white matter, and cerebrospinal fluid [41]. The Diffeomorphic Anatomical Registration Through Exponentiated Lie algebra (DARTEL) tool [42] was used to compute the transformations from individual native space to MNI space and vice-versa. Several sources of spurious or regionally nonspecific variance were removed from the realigned data by regression of nuisance variables, including (i) 24 parameters (6 head motion parameters, 6 head motion parameters one time point before, and the 12 corresponding squared items) obtained by rigid body head motion correction, (ii) the signal averaged over the lateral ventricles, (iii) the signal averaged over a region centered in the

deep cerebral white matter, (iv) and linear and quadratic trends [43]. Finally, temporal filtering (0.01–0.1 Hz) of the time series was performed. To characterize differences in in-scanner micro-head motion, the mean frame-wise displacement (FD), which includes measures of voxel-wise differences in motion in its derivation [44], was used as a measure of the micro-head motion of each subject [43].

■ Degree centrality

Degree centrality (DC) was computed as the number of significant correlations (binarized) of each voxel or as the sum of the weights of the significant connections (weighted) of each voxel [35]. A grey matter mask was used to exclude artifactual correlations from non-gray matter voxels as previously described [33,35].

Within the study mask, individual DC maps were generated in a voxel-wise manner. In brief, we calculated the number of significant correlations or the sum of the weights of significant correlations between the time course of a voxel and that of every other voxel by requiring each connection's strength to exceed a threshold of $r > 0.25$ [29,35,43,45]. Next, the individual-level, voxel-wise DC was converted into a z-score map by subtracting the mean DC across the entire brain and dividing the resulting value by the standard deviation of the whole-brain DC [35,43]. The resulting maps were then registered into MNI space with $3 \times 3 \times 3\text{-mm}^3$ cubic voxels using the transformation information acquired from DARTEL. A smoothing kernel of 8 mm was applied after registration.

Two-sample *t*-tests were performed to analyze the differences between the DC values of the ATSA and HC subjects while accounting for the confounding effects of the education level and Jenkinson's mean FD as recommended by a previous study [45]. The two-sample *t*-test was restricted (masked) to voxels in which the DC values were significant within the HC group or ATSA group using one-sample *t*-tests. For one-sample *t*-tests, a correction for multiple comparisons was applied at the cluster level following Monte Carlo simulations conducted in the 3dFWHMx/3dClustSim modules of AFNI (Version 17.0.18, http://afni.nimh.nih.gov). According to the simulations, a corrected significance level of $P < 0.05$ was obtained with an individual voxel height threshold of $P < 0.001$ (cluster-defining threshold) and a cluster size dependent on the simulation based on the observed smoothness of the data. For two-sample *t*-tests, an overall significance level of $P < 0.05$ corrected for multiple comparisons across the mask (37861 voxels) was calculated using the 3dFWHMx/3dClustSim modules of AFNI (cluster-defining threshold $P = 0.005$, a cluster size ≥ 184, 10,000 Monte Carlo simulations).

■ RSFC networks

To reveal the specific networks influenced by amphetamine-type stimulant abuse, the regions selected based on the results of the DC analyses were used as seed regions for RSFC analyses. For large clusters (e.g., right insula), including several anatomical regions/subregions, seed regions were selected for each anatomical region/subregion. That is, we obtained anterior, middle, and posterior insula seed regions by calculating the intersection between the subregion template of the right insula as defined using the FreeSurfer Atlas (http://surfer.nmr.mgh.harvard.edu/) and the cluster obtained by DC analyses using the "Image Calculator" utility in spm12 (http://www.fil.ion.ucl.ac.uk/spm). The mean time series of each seed region was acquired by averaging the time series of all of the voxels within that region. Pearson's correlation coefficients were computed between the mean time series of the seed region and time series of each voxel in the study mask. The correlation coefficients were converted into *z*-values using Fisher's r-to-z transformation to improve their normality. The *z*-values were analyzed by one-sample *t*-tests to identify brain regions that exhibited significant positive or negative correlations with the seed region within each group. Finally, the *z*-values were analyzed by two-sample *t*-tests to identify brain regions that exhibited significant differences in connectivity with the seed region in the ATSA group and HC group while accounting for the confounding effects of the education level and Jenkinson's mean FD. The two-sample t-test was restricted (masked) to voxels in which connections of the seed region in the network were significant within the HC group or within the ATSA group using one-sample t-tests (cluster-defining threshold $P = 0.001$, cluster size dependent on the simulation based on the observed smoothness of the data). The statistical threshold of the two-sample t-test was set at 3dFWHMx/3dClustSim corrected $P < 0.05$ (cluster-defining threshold $P = 0.005$, cluster size dependent on the simulation based on the observed smoothness of the data for multiple comparison corrections, 10,000 Monte Carlo simulations).

Results

■ Demographic data and head motion

Table 1 shows the characteristics of the subjects and head motion information. The mean ages of the ATSA group and HC group were not significantly different (T = 1.36, P = 0.18). However, the educational level of the ATSAs was significantly lower than that of the HC subjects (*Chi-square* = 21.45, P < 0.001). Therefore, the educational level was included as a covariate in the following analyses. The mean FDs of the ATSA group and HC group were not significantly different (T = 1.49, P = 0.14). However, considering the influence of head motion on intrinsic functional connectivity [46], we also included it as a covariate in the following analyses.

■ Degree centrality

In the HC group, the spatial distribution of the weighted DC was highly localized in the posterior cingulate/ventral precuneus, occipital lobe, middle cingulate cortex (MCC), anterior cingulate cortex/medial prefrontal cortices, lateral prefrontal cortex, inferior parietal regions, and insula (Figure S1). This distribution was similar to that reported in previous studies [33,35]. In the ATSA group, the spatial distribution of the weighted DC was also localized in the abovementioned regions, but the clusters were smaller (Figure S1). In comparison with the HC group, significant decreases in the weighted DC were found in a large cluster that included the right anterior insula, middle insula, posterior insula, and superior temporal gyrus in the ATSA group (Table 2 and Figure 1). The weighted DC in the left inferior temporal gyrus (ITG) of the ATSA group was significantly increased in comparison with that of the HC group (Figure 1). The findings obtained from the binarized graphs were highly similar to those obtained from the weighted graphs and thus are not presented.

■ RSFC networks

We separately selected three subregions of the insula in which the DC was disrupted in the ATSA group as seed regions to reveal the specific networks that were influenced by amphetamine-type stimulant abuse. In general, the spatial distribution of the RSFC of each seed region in the HC group was larger than that of the ATSA group (Figure 2). Functional connectivity for the right middle and posterior insula showed significant group differences (3dClustSim corrected, P < 0.05) (Table 3). Specifically, in the ATSA group, the right middle insula showed a decreased RSFC for a cluster that included the left lingual gyrus and inferior occipital gyrus (3dClustSim corrected P < 0.05, cluster-defining threshold P = 0.005, cluster size > 93 voxels in the mask with 33036 voxels) (Figure 3). The right posterior insula showed a decreased RSFC with

Table 1: Demographic data and subject head motion.

	HC	ATSA
Sample size	21	16
Age (years)	29.52 ± 2.54(25.00-35.00)	28.00 ± 4.24(20.00-38.00)
Education		
Junior high school	1	9
Senior high school	0	2
College degree	7	5
Bachelor degree	13	0
Mean FD	0.06 ± 0.03(0.02-0.13)	0.05 ± 0.02 (0.03-0.11)

Note: Data reflect mean ± standard deviation (range).

Table 2: Group differences in degree centrality between the amphetamine-type stimulant abuser (ATSA) group and the healthy control (HC) group.

Brain region	BA	MNI coordinates	Peak T value	Cluster size
HC > ATSA				
R. insula/superior temporal gyrus	13/41/42/40	57, -24, 15	4.99	272
HC < ATSA				
L. inferior temporal gyrus	20	-39, -12, -36	4.71	273

Note: Threshold is voxel-wise P < 0.005 in conjunction with a cluster-wise P < 0.05 (3dClustSim corrected).

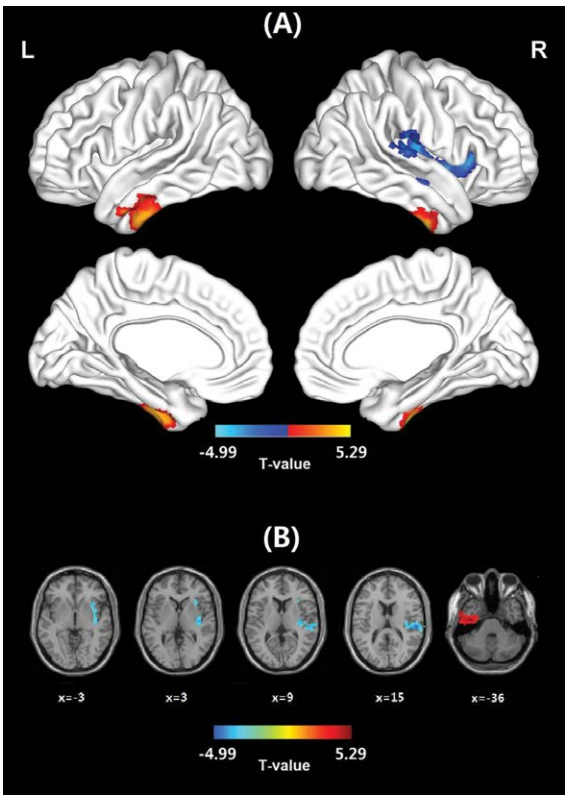

Figure 1: Group differences in degree centrality (DC) between the amphetamine-type stimulant abuser (ATSA) group and the healthy control (HC) group.

Threshold is voxel-wise p<0.005 in conjunction with cluster-wise p<0.05 (3dClustSim corrected). (A) Surface view of the DC group difference. The images were created using BrainNet Viewer (http://www.nitrc.org/projects/bnv/). (B) Slice view of the DC group difference. The images were created using xjview (http://www.alivelearn.net/xjview/).

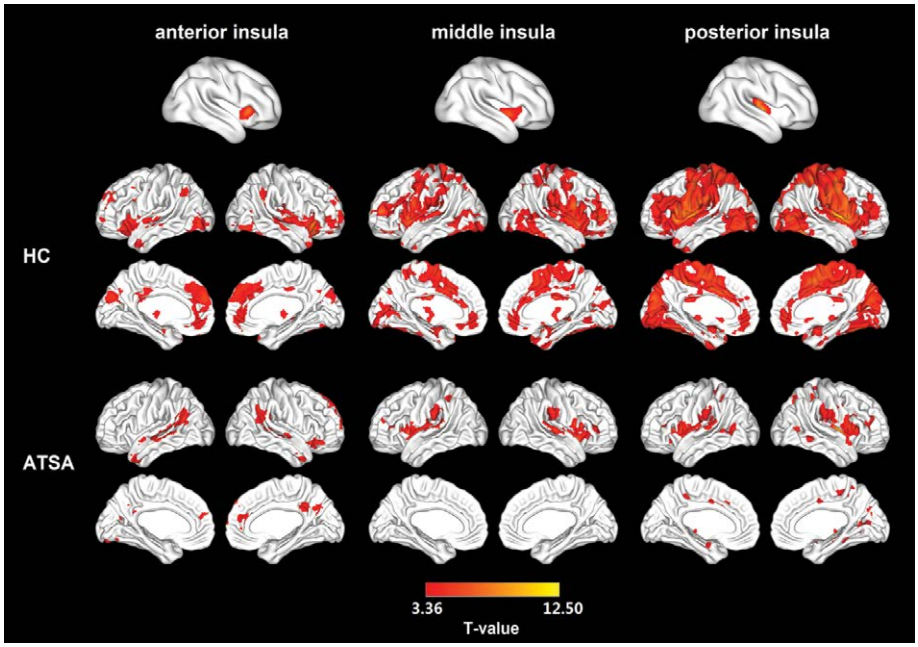

Figure 2: Spatial distribution of the resting-state functional connectivity of three seed regions (the right anterior, middle, and posterior insula) within the healthy control (HC) group and the amphetamine-type stimulant abuser (ATSA) group.

The spatial distribution of the RSFCs was projected onto a surface brain using BrainNet Viewer (http://www.nitrc.org/projects/bnv/).

Table 3: Group differences in functional connectivity between the amphetamine-type stimulant abuser (ATSA) group and the healthy control (HC) group.

Seed ROI	Brain region	BA	MNI coordinates	Peak T value	Cluster size
HC > ATSA					
R. middle insula	L. lingual gyrus/ inferior occipital gyrus	18/17	-6, -99, -18	5.40	203
R. posterior insula	L. middle occipital gyrus/ inferior occipital gyrus/ cuneus	19/18	-42, -93, -6	4.60	467
	B. MPFC/ ACC	11/47/10/32	-18, 51, -9	4.17	330
	R. middle occipital gyrus/ fusiform gyrus	19/37/18	33, -54, -24	3.86	290
	L. precentral gyrus/ postcentral gyrus	6/4	-54, -9, 51	3.99	219
	R. precentral gyrus/ postcentral gyrus	6/4	39, -15, 33	4.51	166
	R. superior temporal gyrus/ insula	22/13	57. -18, 3	4.47	124
	R. inferior occipital gyrus/ middle occipital gyrus	18	24, -87, -12	3.93	99
HC < ATSA					
	none				

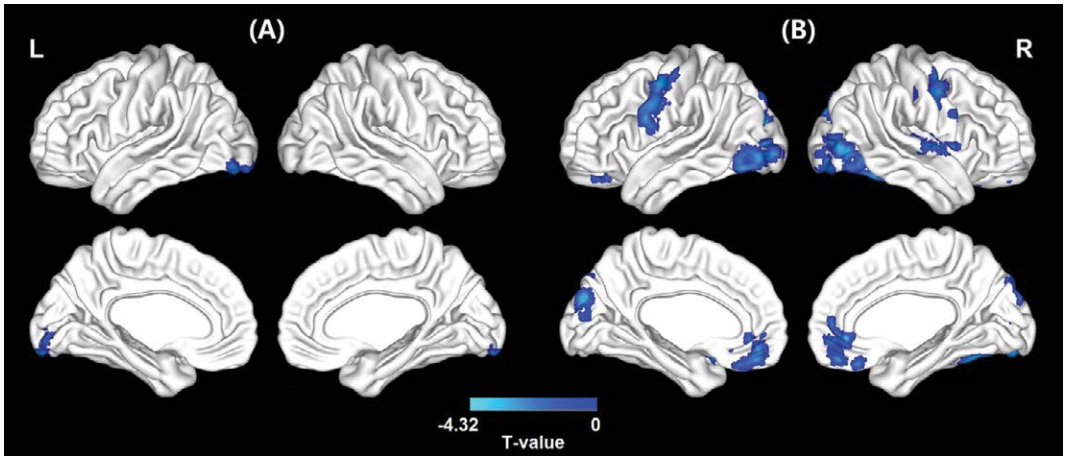

Figure 3: Regions showing altered functional connectivity in the (A) right middle insula and (B) right posterior insula in the amphetamine-type stimulant abuser (ATSA) group compared with the healthy control (HC) group.

Threshold is voxel-wise p<0.005 in conjunction with cluster-wise p<0.05 (3dClustSim corrected). The images were created using BrainNet Viewer (http://www.nitrc.org/projects/bnv/).

a cluster that included the MPFC and anterior cingulate cortex (ACC), bilateral precentral gyrus and postcentral gyrus, and bilateral occipital lobe (3dClustSim corrected $P < 0.05$, cluster-defining threshold p = 0.005, cluster size >118 voxels in the mask with 23398 voxels) **(Figure 3)**. No increased functional connectivity was found in the ATSA group compared with the HC group. No significant difference between the HC group and ATSA group was detected when the left ITG was used as the seed region for RSFC (3dClustSim corrected $P < 0.05$).

Discussion

In the current study, we demonstrated that the resting-state brain functional architecture was disrupted in ATSAs. The ATSA group showed a decreased spatial distribution of weighted DC, especially in a large cluster that included the right anterior insula, middle insula, and posterior insula. Furthermore, seed-based RSFC analyses revealed that the decreased RSFC related to the right middle and posterior insula involved regions in the MPFC and visual and sensorimotor cortices in the ATSA group.

The insula is a brain structure with a complex functional and structural organization. Recent studies employing a diverse range of methodological approaches appear to converge on the functional parcellation of the insula into at least 3 functionally distinct subregions [47-52]. The anterior insula is involved in interoceptive processes, including pain sensing and emotional processing [53], and plays an important role in social emotions [54] and decision-making [55-57]. The middle insula

clusters are associated with sensory perception, somesthesis, and interoception [58]. The posterior insula is most strongly associated with somatosensory, vestibular, and motor integration [59]. In addition, the posterior insula also serves as an integrative heteromodal association area for information received by the five senses (gustatory, olfactory, auditory, somesthetic and visual) [60].

Previous functional and structural studies have suggested a probable role for the insula in drug abuse and addiction [59,61,62]. In comparison with healthy controls, methamphetamine-dependent subjects exhibited an attenuated anterior insula response [63-65] and reduced activity in the dorsal and posterior insula when performing decision-making tasks [65-67]. Dysfunction in the insula cortices of abstinent methamphetamine abusers contributes to impaired vigilance [68] and cognitive control deficits [69]. Hypoactivation of the insula in methamphetamine abusers suggests compromised emotional awareness to threatening scenes and empathy for another's pain [70]. In addition to functional abnormalities in the insula, ATSAs have been found to possess structural abnormalities in the insula, including a decreased cortical density, grey and white matter volume, and cortical thickness [71-77]. Our finding that the DC in the insula of the ATSA group was decreased suggests that there is less interaction between the right insula and other brain regions in ATSAs during the resting state, thus providing new evidence of insula dysfunction associated with amphetamine-type stimulant abuse from a brain network perspective using resting-state fMRI.

Using seed-based RSFC, we showed that ATSAs had altered functional connectivity between the posterior insular and medial prefrontal cortex, in line with the hypothesis that cocaine dependence is related to an altered functional interaction of the insular cortex with prefrontal networks [78]. The posterior insula showed decreased connectivity strength with the more rostral part of the MPFC, including the medial orbitofrontal cortex (OFC). In comparison with the healthy control group, cocaine-addicted subjects showed a significant increase in metabolic response in the right medial prefrontal cortex [79,80]. The orbitofrontal cortex has also been reported to show hypoactivity after detoxification [81]. In addition to functional alterations, imaging studies using MRI have documented morphological abnormalities in the medial OFC of substance-dependent individuals [71,82-84]. Our findings are consistent with these previous studies. Similar to our findings, abnormal insula-MPFC functional connectivity has also been reported in smoking studies, e.g., a weakened right anterior insula–ventral MPFC functional circuit in smoking abstinent subjects [85]. This similarity suggests that amphetamine-type stimulants may interfere with functional networks similar to smoking. In brief, the decreased insula-MPFC RSFC reported in this study provides new evidence for dysfunction of the prefrontal-insula circuit in substance addiction.

We also found that the right middle and posterior insula in the ATSAs showed reduced functional connectivity with the visual cortex and its association cortices. The RSFC between the posterior insula and occipital cortices has been found using resting-state fMRI [50,52,58,86,87]. We speculate that these abnormalities observed in ATSAs may be correlated with psychotic symptoms, such as visual hallucinations, which have been documented in previous studies [88]. Future studies should aim to illuminate the relationship between changes in functional connectivity and psychotic symptoms in ATSAs. In addition, we found reduced functional connectivity between the posterior insula and sensorimotor cortices. Cauda et al. suggested that the links between the middle-posterior insula and premotor, sensorimotor and supplementary motor cortices indicated the insular role of sensorimotor integration [50]. We speculate that these reduced functional connections may reflect the reduced functional integration between multiple senses and may be related to the perturbed homeostatistic steady state suggested in drug addiction [89]. However, this speculation needs to be tested in future stuies.

Another finding in this study is the increased DC in the left inferior temporal gyrus. The left inferior temporal gyrus is likely involved in retrieval load [90] and visual perception [91,92]. The inferior temporal gyrus shows a significantly greater response to novel versus familiar stimuli across visual, auditory and tactile sensory modalities [93]. A previous study also discovered that in students who were referred to a college alcohol and drug assistance program, polydrug (containing club drugs such as methamphetamine, LSD and ketamine) cues produced significantly greater left inferior temporal gyrus activity compared with neutral cues [94]. Cocaine-dependent participants had increased neural functioning of the left inferior

temporal gyrus in the "reward" compared to the "no-reward" condition during reward-based spatial learning (a form of episodic memory) [95]. In comparison to a placebo, the left inferior temporal gyrus of those who used designer drugs containing benzylpiperazine (a worldwide safe and legal alternative to illicit recreational drugs, such as MDMA and methamphetamine) showed decreased activation in a Stroop task, especially during the incongruent condition [96]. Therefore, we speculate that the ATSAs might pay more attention to thinking about obtaining and using amphetamine-type stimulants, and thus show higher resting-state activity of the left inferior temporal gyrus.

The present study has several limitations. First, only male participants were recruited to eliminate the confounding factor of sex differences. After all, some factors could potentially vary the developmental timecourses of vulnerability to amphetamine toxicity in different genders [5]. Therefore, we cannot infer the RSFC pattern in female ATSAs based on the current findings. Second, considering small differences in head motion were sufficient to produce specific effects in seed-based functional connectivity maps [46], the current results could not completely eliminate the impact of head motion, even after we included it as a covariate. Third, the ATSAs were scanned during substance withdrawal, whereas the HCs were not, so we were not able to absolutely exclude the influence of smoking, drinking or caffeine. In addition, the sample size of this study was relative small due to the practical difficulties in recruitment of ATSAs in a clinical hospital, such as difficulty in building cooperation between patients and researchers and difficulty in obtaining informed consent from patients or their families. The relative smaller sample size may also account for the insignificant group differences while using the left ITG as the seed region for RSFC analyses. Therefore, the findings obtained in the current study need to be validated in studies with larger sample sizes in the future. Finally, in this study, we were not able to exclude the possibility that the abnormal resting-state activity observed in the ATSAs was independent or dependent on some clinical characteristics, such as depression, anxiety, or impulsivity. For example, a recent study that compared insular RSFC of drug-naïve major depressive disorder (MDD) and healthy controls found that the RSFCs between the right insula and left middle frontal gyrus and right middle occipital gyrus were decreased in the MDD patients [86], suggesting that depression may lead to disrupted insula RSFC. In a future study, it is necessary to measure these clinical indices to explore the correlation between the clinical characteristics and insular resting-state functional networks or controlling individual differences in various clinical symptoms.

Conclusions

In the present study, we demonstrated a disrupted resting-state brain functional architecture in ATSAs from a new brain network perspective using resting-state fMRI. The ATSA group showed decreased DC in the right insula. The decreased functional connectivity in the insula may have resulted from the decreased functional interaction between the insula and MPFC as well as visual and sensorimotor cortices. These results provide important new information on the manner in which amphetamine-type stimulants alter resting state brain activity in male abusers. In addition, these findings should facilitate the development of improved biomarkers for amphetamine-type stimulant abuse.

Acknowledgements

This research was supported by the National Key Technology R&D Program in the 12th Five-Year Plan of China (2012BAI01B07).

Author contributions

Qun Chen, Zhan-Jiang Li, Xiao-nian Luo and Yuan Zhou provided the theoretical framework and intellectual content guidance. Kai-Juan Yan and Chen-xiao Fan collected all data. Dang Zheng performed the data analysis guided by Yuan Zhou. Qun Chen and Yuan Zhou were responsible for the interpretation of the results. Qun Chen, Dang Zheng and Shaojuan Cui contributed to the writing of the manuscript. Qun Chen, Dang Zheng, Shaojuan Cui, Kai-Juan Yan, Chen-xiao Fan, Guo-fu Zhang, Le Xiao, Yan Li, Xiao-fei Yuan, Kankan Xie, Yaqiong Li, Xiao-nian Luo, Yuan Zhou, Zhan-Jiang Li critically reviewed the content of the manuscript and approved the final version for publication.

Conflict of interest

The authors have declared that no competing interests exist.

References

1. Sun HQ, Bao YP, Zhou SJ, *et al.* The new pattern of drug abuse in China. *Curr. Opin. Psychiatry* 27(4), 251-255 (2014).
2. Jerry J, Collins G, Streem D. Synthetic legal intoxicating drugs: the emerging 'incense' and 'bath salt' phenomenon. *Cleve. Clin. J. Med* 79(4), 258-264 (2012).
3. Barr AM, Panenka WJ, MacEwan GW, *et al.* The need for speed: an update on methamphetamine addiction. *J. Psychiatry. Neurosci* 31(5), 301-313 (2006).
4. Scott JC, Woods SP, Matt GE, *et al.* Neurocognitive effects of methamphetamine: a critical review and meta-analysis. *Neuropsychol. Rev* 17(3), 275-297 (2007).
5. Berman S, O'Neill J, Fears S, *et al.* Abuse of amphetamines and structural abnormalities in the brain. *Ann. NY. Acad. Sci* 1141(1), 195-220 (2008).
6. Paulus MP, Tapert SF, Schuckit MA. Neural activation patterns of methamphetamine-dependent subjects during decision making predict relapse. *Arch. Gen. Psychiatry* 62(7), 761-768 (2005).
7. Raichle ME, Mintun MA. Brain work and brain imaging. *Annu. Rev. Neurosci* 29(1), 449-476 (2006).
8. Fox MD, Raichle ME. Spontaneous fluctuations in brain activity observed with functional magnetic resonance imaging. *Nat. Rev. Neurosci* 8(9), 700-711 (2007).
9. Deco G, Jirsa VK, McIntosh AR. Emerging concepts for the dynamical organization of resting-state activity in the brain. *Nat. Rev. Neurosci* 12(1), 43-56 (2011).
10. Rosazza C, Minati L. Resting-state brain networks: literature review and clinical applications. *Neurol. Sci* 32(5), 773-85 (2011).
11. Fornito A, Bullmore ET. What can spontaneous fluctuations of the blood oxygenation-level-dependent signal tell us about psychiatric disorders? *Curr. Opin. Psychiatry* 23(3), 239-249 (2010).
12. Ma N, Liu Y, Li N, *et al.* Addiction related alteration in resting-state brain connectivity. *Neuroimage* 49(1), 738-744 (2010).
13. Yuan K, Qin W, Dong M, *et al.* Combining spatial and temporal information to explore resting-state networks changes in abstinent heroin-dependent individuals. *Neurosci. Lett* 475(1), 20-24 (2010).
14. Qiu YW, Han LJ, Lv XF, *et al.* Regional homogeneity changes in heroin-dependent individuals: resting-state functional MR imaging study. *Radiology* 261(2), 551-559 (2011).
15. Zhang Y, Gong J, Xie C, *et al.* Alterations in brain connectivity in three sub-regions of the anterior cingulate cortex in heroin-dependent individuals: Evidence from resting state fMRI. *Neuroscience* 284(1), 998-1010 (2015).
16. Hong LE, Gu H, Yang Y, *et al.* Association of nicotine addiction and nicotine's actions with separate cingulate cortex functional circuits. *Arch. Gen. Psychiatry* 66(4), 431-441 (2009).
17. Sutherland MT, Carroll AJ, Salmeron BJ, *et al.* Insula's functional connectivity with ventromedial prefrontal cortex mediates the impact of trait alexithymia on state tobacco craving. *Psychopharmacology* 228(1), 143-155 (2013).
18. Li S, Yang Y, Hoffmann E, *et al.* CYP2A6 Genetic Variation Alters Striatal-Cingulate Circuits, Network Hubs, and Executive Processing in Smokers. *Biological. Psychiatry* 81(7), 554-563 (2017).
19. Sutherland MT, McHugh MJ, Pariyadath V, *et al.* Resting state functional connectivity in addiction: lessons learned and a road ahead. *Neuroimage* 62(4), 2281-2295 (2012).
20. Gu H, Salmeron BJ, Ross TJ, *et al.* Mesocorticolimbic circuits are impaired in chronic cocaine users as demonstrated by resting-state functional connectivity. *Neuroimage* 53(2), 593-601 (2010).
21. Hu Y, Salmeron BJ, Gu H, *et al.* Impaired functional connectivity within and between frontostriatal circuits and its association with compulsive drug use and trait impulsivity in cocaine addiction. *JAMA. Psychiatry*; 72(6), 584-592 (2015).
22. Baler RD, Volkow ND. Drug addiction: the neurobiology of disrupted self-control. *Trends. Mol. Med* 12(12), 559-566 (2006).
23. Carhart-Harris RL, Murphy K, Leech R, *et al*. The Effects of Acutely Administered 3,4-Methylenedioxymethamphetamine on Spontaneous Brain Function in Healthy Volunteers Measured with Arterial Spin Labeling and Blood Oxygen Level-Dependent Resting State Functional Connectivity. *Biol. Psychiatry* 78(8), 554-562 (2015).
24. Kohno M, Morales AM, Ghahremani DG, *et al*. Risky decision making, prefrontal cortex, and mesocorticolimbic functional connectivity in methamphetamine dependence. *JAMA. Psychiatry* 71(7), 812-820 (2014).
25. Roseman L, Leech R, Feilding A, *et al.* The effects of psilocybin and MDMA on between-network resting state functional connectivity in healthy volunteers. *Front. Hum. Neurosci* 8(1), 204 (2014).
26. Dean AC, Kohno M, Morales AM, *et al*. Denial in methamphetamine users: Associations with cognition and functional connectivity in brain. *Drug. Alcohol. Depend* 151, 84-91 (2015).
27. Wilkins C, Reilly J, Rose E, *et al.* The Socio-Economic impact of amphetamine type stimulants in New Zealand. Centre for Social and Health Outcomes Research and Evaluation (SHORE) Massey University, Auckland (2004).
28. Kohno M, Morales AM, Ghahremani DG, et al. Risky decision making, prefrontal cortex, and mesocorticolimbic functional connectivity in methamphetamine dependence. *JAMA. psychiatry* 71(7), 812-820 (2014).
29. Buckner RL, Sepulcre J Talukdar T, *et al.* Cortical hubs revealed by intrinsic functional connectivity: mapping, assessment of stability, and relation to Alzheimer's disease. *J. Neurosci*; 29(6), 1860-1873 (2009).
30. Fransson P, Aden U, Blennow M, *et al.* The functional architecture of the infant brain as revealed by resting-state fMRI. *Cereb. Cortex* 21(1), 145-154 (2011).
31. Lord LD, Allen P, Expert P, *et al.* Characterization of the anterior cingulate's role in the at-risk mental state using graph theory. *Neuroimage* 56(3), 1531-15399 (2011).
32. Di Martino A, Zuo XN, Kelly C, *et al.* Shared and distinct intrinsic functional network centrality in autism and attention-deficit/hyperactivity disorder. *Biol. Psychiatry* 74(8), 623-632 (2013).
33. Zhou Y, Wang Y, Rao LL, *et al.* Disrutpted resting-state functional architecture of the brain after 45-day simulated microgravity. *Front. Behav. Neurosci* 8(1), 200 (2014).
34. Tomasi D, Volkow ND. Functional connectivity hubs in the human brain. *Neuroimage* 57(3), 908-917 (2011).
35. Zuo XN, Ehmke R, Mennes M, *et al.* Network centrality in the human functional connectome. *Cereb. Cortex* 22(8), 1862-1875 (2012).
36. Association AP Diagnostic and statistical manual of mental disorders: DSM-IV-TR®. *American Psychiatric Pub*. 2000.
37. Luo W, Guo CX, Han de L, *et al*. Reliability and validity of Chinese version of the Addiction Severity Index among drug users in the community. *Biomed. Environ. Sci* 25(6), 684-689 (2012).
38. McLellan, AT, Kushner H, Metzger D, *et al.* The Fifth Edition of the Addiction Severity Index. *J Subst. Abuse. Treat* 9(3), 199-213 (1992).
39. Chao-Gan Y, Yu-Feng Z. DPARSF: A MATLAB Toolbox for "Pipeline" Data Analysis of Resting-State fMRI. *Front. Syst. Neurosci* 4(1), 13 (2010).

40. Song XW, Dong ZY, Long XY, *et al.* REST: a toolkit for resting-state functional magnetic resonance imaging data processing. *PLoS. One* 6(9), e25031 (2011).

41. Ashburner J, Friston KJ. Unified segmentation. *Neuroimage* 26(3), 839-851 (2005).

42. Ashburner J (2007) A fast diffeomorphic image registration algorithm. *Neuroimage* 38(1), 95-113 (2007).

43. Yan CG, Craddock RC, Zuo XN, *et al.* Standardizing the intrinsic brain: towards robust measurement of inter-individual variation in 1000 functional connectomes. *Neuroimage* 80(1), 246-262 (2013).

44. Jenkinson M, Bannister P, Brady M, *et al.* Improved optimization for the robust and accurate linear registration and motion correction of brain images. *Neuroimage* 17(2), 825-841 (2002).

45. Yan CG, Cheung B, Kelly C, *et al.* A comprehensive assessment of regional variation in the impact of head micromovements on functional connectomics. *Neuroimage* 76(1), 183-201 (2013).

46. Van Dijk KR, Sabuncu MR, Buckner RL. The influence of head motion on intrinsic functional connectivity MRI. *Neuroimage* 59(1), 431-438 (2012).

47. Nanetti L, Cerliani L, Gazzola V, *et al.* Group analyses of connectivity-based cortical parcellation using repeated k-means clustering. *Neuroimage* 47(4), 1666-1677 (2009).

48. Kurth F, Eickhoff SB, Schleicher A, *et al.* Cytoarchitecture and probabilistic maps of the human posterior insular cortex. *Cereb. Cortex* 20(6), 1448-1461 (2010).

49. Nelson SM, Dosenbach NU, Cohen AL, *et al.* Role of the anterior insula in task-level control and focal attention. *Brain. Struct. Funct* 214(5-6), 669-680 (2010).

50. Cauda F, D'Agata F, Sacco K, *et al.* Functional connectivity of the insula in the resting brain. *Neuroimage* 55(1), 8-23 (2011).

51. Deen B, Pitskel, NB, Pelphrey KA (2011) Three systems of insular functional connectivity identified with cluster analysis. *Cereb. Cortex* 21(7), 1498-1506 (2011).

52. Chang LJ, Yarkoni T, Khaw MW, *et al.* Decoding the role of the insula in human cognition: functional parcellation and large-scale reverse inference. *Cereb. Cortex* 23(3), 739-749 (2013).

53. Lindquist KA, Wager TD, Kober H, *et al.* The brain basis of emotion: a meta-analytic review. *Behav. Brain. Sci* 35(3), 121-143 (2012).

54. Lamm C, Singer T. The role of anterior insular cortex in social emotions. *Brain. Struct. Funct* 214(5-6), 579-591 (2010).

55. Sanfey AG. Social decision-making: insights from game theory and neuroscience. *Science* 318(5850), 598-602 (2007).

56. Thielscher A, Pessoa L. Neural correlates of perceptual choice and decision making during fear-disgust discrimination. *J. Neurosci* 27(11), 2908-2917 (2007).

57. Bossaerts P. Risk and risk prediction error signals in anterior insula. *Brain. Structure. and Function* 214(5-6), 645-653 (2010).

58. Kelly C, Toro R, Di Martino A, *et al.* A convergent functional architecture of the insula emerges across imaging modalities. *Neuroimaging* 61(4), 1129-1142 (2012).

59. Naqvi NH, Bechara A. The hidden island of addiction: the insula. *Trends. Neurosci* 32(1), 56-67 (2009).

60. Flynn FG. Anatomy of the insula functional and clinical correlates. *Aphasiology* 13(1), 55-78 (1999).

61. Wilson SJ, Sayette MA, Fiez JA. Prefrontal responses to drug cues: a neurocognitive analysis. *Nat. Neurosci* 7(3), 211-214 (2004).

62. Heinz A, Beck A, Grusser SM, *et al.* Identifying the neural circuitry of alcohol craving and relapse vulnerability. *Addict. Biol* 14(1), 108-118 (2009).

63. May AC, Stewart JL, Migliorini R, *et al.* Methamphetamine dependent individuals show attenuated brain response to pleasant interoceptive stimuli. *Drug. Alcohol. Depend* 131(3), 238-246 (2013).

64. Stewart JL, May AC, Poppa T, *et al.* You are the danger: attenuated insula response in methamphetamine users during aversive interoceptive decision-making. *Drug. Alcohol. Depend* 142, 110-119 (2014).

65. Gowin JL, Stewart JL, May AC, *et al.* Altered cingulate and insular cortex activation during risk-taking in methamphetamine dependence: losses lose impact. *Addiction* 109(2), 237-247 (2014).

66. Paulus MP, Tapert SF, Schuckit MA. Neural activation patterns of methamphetamine-dependent subjects during decision making predict relapse. *Arch. Gen. Psychiatry* 62(7), 761-768 (2005).

67. Stewart JL, Connolly CG, May AC, *et al.* Striatum and insula dysfunction during reinforcement learning differentiates abstinent and relapsed methamphetamine-dependent individuals. *Addiction* 109(3), 460-471 (2014).

68. London ED, Berman SM, Voytek B, *et al.* Cerebral metabolic dysfunction and impaired vigilance in recently abstinent methamphetamine abusers. *Biol. Psychiatry* 58(10), 770-778 (2005).

69. Nestor LJ, Ghahremani DG, Monterosso J, *et al.* Prefrontal hypoactivation during cognitive control in early abstinent methamphetamine-dependent subjects. *Psychiatry. Res* 194(3), 287-295 (2011).

70. Kim YT, Son HJ, Seo JH, *et al.* The differences in neural network activity between methamphetamine abusers and healthy subjects performing an emotion-matching task: functional MRI study. *NMR. Biomed* 24(10), 1392-1400 (2011).

71. Franklin TR, Acton PD, Maldjian JA, *et al.* Decreased gray matter concentration in the insular, orbitofrontal, cingulate, and temporal cortices of cocaine patients. *Biol. Psychiatry* 51(2), 134-142 (2002).

72. Makris N, Gasic GP, Kennedy DN, *et al.* Cortical thickness abnormalities in cocaine addiction--a reflection of both drug use and a pre-existing disposition to drug abuse? *Neuron* 60(1), 174-188 (2008).

73. Schwartz DL, Mitchell AD, Lahna DL, *et al.* Global and local morphometric differences in recently abstinent methamphetamine-dependent individuals. *Neuroimage* 50(4), 1392-1401 (2010).

74. Gardini S, Venneri A. Reduced grey matter in the posterior insula as a structural vulnerability or diathesis to addiction. *Brain. Res. Bull* 87(2-3), 205-211 (2012).

75. Morales AM, Lee B, Hellemann G, *et al.* Gray-matter volume in methamphetamine dependence: cigarette smoking and changes with abstinence from methamphetamine. *Drug. Alcohol. Depend* 125(3), 230-238 (2012).

76. Moreno-Lopez L, Catena A, Fernandez-Serrano MJ, *et al.* Trait impulsivity and prefrontal gray matter reductions in cocaine dependent individuals. *Drug. Alcohol. Depend* 125(3), 208-214 (2012).

77. Tanabe J, York P, Krmpotich T, *et al.* Insula and orbitofrontal cortical morphology in substance dependence is modulated by sex. *AJNR. Am. J. Neuroradiol* 34(6), 1150-1156 (2013).

78. Cisler JM, Elton A, Kennedy AP, *et al.* Altered functional connectivity of the insular cortex across prefrontal networks in cocaine addiction. *Psychiatry. Res* 213(1), 39-46 (2013).

79. Volkow ND, Wang GJ, Ma Y, *et al.* Activation of orbital and medial prefrontal cortex by methylphenidate in cocaine-addicted subjects but not in controls: relevance to addiction. *J. Neurosci* 25(15), 3932-3939 (2005).

80. Schoenbaum G, Shaham Y. The role of orbitofrontal cortex in drug addiction: a review of preclinical studies. *Biological. Psychiatry* 63(3), 256-262 (2008).

81. Dom, G, Sabbe, B, Hulstijn, W, *et al.* Substance use disorders and the orbitofrontal cortex: systematic review of behavioural decision-making and neuroimaging studies. *Br. J. Psychiatry* 187(1), 209-220 (2005).

82. De Bellis MD, Narasimhan A, Thatcher DL, *et al.* Prefrontal cortex, thalamus, and cerebellar volumes in adolescents and young adults with adolescent-onset alcohol use disorders

and comorbid mental disorders. *Alcohol. Clin. Exp. Res* 29(9), 1590-600 (2005).

83. Tanabe J, Tregellas JR, Dalwani M, *et al.* Medial orbitofrontal cortex gray matter is reduced in abstinent substance-dependent individuals. *Biol. Psychiatry* 65(2), 160-164 (2009).

84. Kuhn S, Schubert F, Gallinat J. Reduced thickness of medial orbitofrontal cortex in smokers. *Biol Psychiatry* 68(11), 1061-1065 (2010).

85. Sutherland MT, Carroll AJ, Salmeron BJ, *et al.* Insula's functional connectivity with ventromedial prefrontal cortex mediates the impact of trait alexithymia on state tobacco craving. *Psychopharmacology* (Berl) 228(1), 143-155 (2013).

86. McGlone F, Kelly EF, Trulsson M, *et al.* Functional neuroimaging studies of human somatosensory cortex. *Behav. Brain. Res* 135(1-2), 147-158 (2002).

87. Taylor KS, Seminowicz DA, Davis KD. Two systems of resting state connectivity between the insula and cingulate cortex. *Hum. Brain. Mapp* 30(9), 2731-2745 (2009).

88. Hides L, Dawe S, McKetin R, *et al.* Primary and substance-induced psychotic disorders in methamphetamine users. *Psychiatry. Res* 226(1), 91-96 (2015).

89. Paulus MP, Tapert SF, Schulteis G. The role of interoception and alliesthesia in addiction. *Pharmacol. Biochem. Behav* 94(1), 1-7 (2009).

90. Walsh ND, Phillips ML. Interacting outcome retrieval, anticipation, and feedback processes in the human brain. *Cerebral. Cortex* bhp098 (2009).

91. Ishai A, Ungerleider LG, Martin A, *et al.* Distributed representation of objects in the human ventral visual pathway. *Proceedings. of. the National Academy of Sciences* 96(16), 9379-9384 (1999).

92. Herath P, Kinomura S, Roland PE. Visual recognition: evidence for two distinctive mechanisms from a PET study. *Human. Brain. mapping* 12(2), 110-119 (2001).

93. Downar J, Crawley AP, Mikulis DJ, *et al.* A cortical network sensitive to stimulus salience in a neutral behavioral context across multiple sensory modalities. *J. Neurophysiol* 87(1), 615-620 (2002).

94. Ray S, Hanson C, Hanson SJ, *et al.* fMRI BOLD response in high-risk college students (part 1): during exposure to alcohol, marijuana, polydrug and emotional picture cues. *Alcohol. And. Alcoholism* 45(5), 437-443 (2010).

95. Tau GZ, Marsh R, Wang Z, *et al.* Neural correlates of reward-based spatial learning in persons with cocaine dependence. *Neuropsychopharmacology* 39(3), 545-555 (2014).

96. Curley LE, Kydd RR, Robertson MC, *et al.* Acute effects of the designer drugs benzylpiperazine (BZP) and trifluoromethylphenylpiperazine (TFMPP) using functional magnetic resonance imaging (fMRI) and the Stroop task—a pilot study. *Psychopharmacology* 232(16), 2969-2980 (2015).